アカデミックプログラム［B講演］ | 05. 物理化学—反応：口頭B講演

2025年3月28日(金) 9:00 ~ 11:30 [C]C401(第2学舎 2号館 [4階] C401)

[[C]C401-3am] 05. 物理化学—反応

座長：村松 悟、長澤 裕

英語
9:00 ~ 9:20
[[C]C401-3am-01]
低温イオン移動度質量分析による2価金属イオンとクラウンエーテルの気相錯体の構造の研究
○伊藤 亮佑[1]、大下 慶次郎[1]、美齊津 文典[1] (1. 東北大院理)

英語
9:20 ~ 9:40
[[C]C401-3am-02]
衝突誘起解離およびイオン移動度質量分析を用いたプロトン付加アミノ桂皮酸の長距離プロトン移動の研究
○角田 健吾[1]、布施 大輝[1]、浅川 大樹[2]、大下 慶次郎[1]、美齊津 文典[1] (1. 東北大学大学院理学研究科、2. 産業技術総合研究所)

英語
9:40 ~ 10:00
[[C]C401-3am-03]
イオン移動度質量分析によるランタノイドハロゲン化物クラスター負イオンの幾何構造の研究：ランタノイド収縮に伴うイオン半径変化と構造の関係
○中島 優斗[1]、Patrick Weis[2]、Florian Weigend[2]、Marcel Lukanowski[2]、美齊津 文典[1]、Manfred Kappes[2] (1. 東北大、2. カールスルーエ工科大)

10:00 ~ 10:10
休憩

日本語
10:10 ~ 10:30
[[C]C401-3am-04]
液膜ジェット技術を用いたマイクロ秒溶液混合技術の開発
○遠藤 友随[1]、板倉 隆二[1] (1. 量子科学技術研究開発機構)

日本語
10:30 ~ 10:50
[[C]C401-3am-05]
プラスチック分解物の高選択的かつ高効率な酸化反応を加速させるヘマタイト光電極の設計
○村尾 智央[1]、隈部 佳孝[2]、立川 貴士[1,2] (1. 神戸大院理、2. 神戸大分子フォト)

英語
10:50 ~ 11:10
[[C]C401-3am-06]
ペロブスカイトナノ結晶—シアニン色素間のエネルギー移動における結晶サイズ依存性
○山口 哲生[1]、福増 知也[1]、久保 直輝[1]、増尾 貞弘[1] (1. 関西学院大学)

英語
11:10 ~ 11:30

[[C]C401-3am-07]

真空紫外光電子分光で観るアデノシン誘導体における超高速光物理過程

○古賀 雅史[1]、Do Hyung Kang[2]、Zachary Heim[2]、Neal Haldar[2]、Daniel Neumark[2] (1. 分子研、2. UC Berkeley)

Gas-Phase Structures of Crown Ether Complexes with Divalent Metal Cations Studied by Cryogenic Ion Mobility–Mass Spectrometry

(*Graduate School of Science, Tohoku University*)
○Ryosuke Ito, Keijiro Ohshimo, Fuminori Misaizu
Keywords: Ion Mobility–Mass Spectrometry; Crown Ether; Conformer; Ion Selectivity

Crown ethers are crucial in host-guest chemistry due to their remarkable ability to encapsulate guest ions efficiently and selectively. Previously, we studied the conformations of dibenzo-24-crown-8 (DB24C8) complexes with alkali metal ions using cryogenic ion mobility–mass spectrometry (IM-MS) and confirmed the coexistence of open and closed conformers with long and short distances between the two benzene rings.[1] In this study, we analyzed the conformations of DB24C8 complexes with alkaline earth metal ions (Mg^{2+}, Ca^{2+}, Sr^{2+}, Ba^{2+}) and transition metal ions (Fe^{2+}, Ni^{2+}, Zn^{2+}), focusing on how ionic radii and charges of the guest ions affect the conformations of the complexes.

For alkaline earth metal ion complexes, both closed and open conformers were observed at 86 K. Relative abundances of the conformers depended on the ionic radii of the guest ions, resembling the behavior observed with alkali metal ions. Among these, Ba^{2+}(DB24C8) exhibited a structure highly similar to K^{+}(DB24C8) because K^{+} and Ba^{2+} have close ionic radii (1.35 Å and 1.38 Å) (Fig. 1). In the closed conformers of these complexes, the distances between the centers of the two benzene rings were close (3.88 Å and 3.72 Å). These structural similarities suggest that the ionic radius of the guest ion predominantly governs the conformation of the DB24C8 complexes. In contrast, transition metal ion complexes exhibited diverse conformations, even among metals with similar ionic radii. The closed conformer was predominant in the Fe^{2+} complex, the open conformer was predominant in the Ni^{2+} complex, and both closed and open conformers were observed in the Zn^{2+} complex. Quantum chemical calculations suggested that the ions had different coordination numbers, which was responsible for the observed conformational differences.

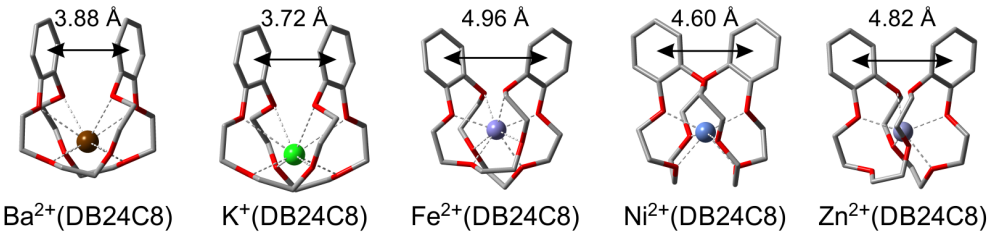

Fig. 1. The most stable closed conformers of DB24C8 complexes with Ba^{2+}, K^{+}, Fe^{2+}, Ni^{2+}, and Zn^{2+} obtained by B3LYP-D3(BJ)/def2-SVP level at 86 K. Hydrogen atoms are not shown for clarity.

1) K. Ohshimo, X. He, R. Ito, K. Tsunoda, S. Tainaka, F. Misaizu, *EPJ Techn. Instrum.* **2023**, *10*, 11.

Long-Distance Proton Transfer in Protonated Aminocinnamic Acid Studied by Collision-Induced Dissociation and Ion Mobility-Mass Spectrometry

([1]*Graduate School of Science, Tohoku University*, [2]*AIST*) ○Kengo Tsunoda,[1] Daiki Fuse,[1] Daiki Asakawa,[2] Keijiro Ohshimo,[1] Fuminori Misaizu[1]

Keywords: ion mobility-mass spectrometry; collision-induced dissociation; proton transfer; vehicle mechanism

Intramolecular proton transfer reactions proceed in protonated *p*-aminobenzoic acid (PABA·H^+) between two isomers: N-protomer, where the proton is added to the amino group's nitrogen, and O-protomer, where the proton is added to the carboxyl group's oxygen. By ion mobility-mass spectrometry (IM-MS), ions can be separated based on their collision cross sections (CCSs) with buffer gas. We recently demonstrated that a proton was transported from N-protomer to O-protomer in PABA·H^+ by a collision with ammonia using IM-MS[1]. The proton transfer was examined in this study for the protonated aminocinnamic acid (ACA·H^+), which has a longer distance between the amino and carboxyl groups compared to PABA·H^+ (**Fig. 1(a)**). As a result, similar proton transfer was also observed for ACA·H^+, however, unlike PABA·H^+, not only the O-protomer but also the C-protomer could be formed as the current reaction products. It was not possible to separate the O- and C-protomers in IM-MS due to their close CCSs (**Fig. 1(b)**). Therefore, collision-induced dissociation (CID) with argon gas was employed after ion mobility analysis to assign the reaction products based on their fragmentation patterns. CID results indicated the release of H_2O at relatively low collision energies, with subsequent CO loss observed at higher energies (**Fig. 1(c)**). Quantum chemical calculations revealed that the transition state barrier for H_2O loss from the O-protomer is lower than from the C-protomer, and only the O-protomer leads to subsequent CO loss. These suggest the predominant formation of O-protomer in the proton transfer reactions within ACA·H^+.

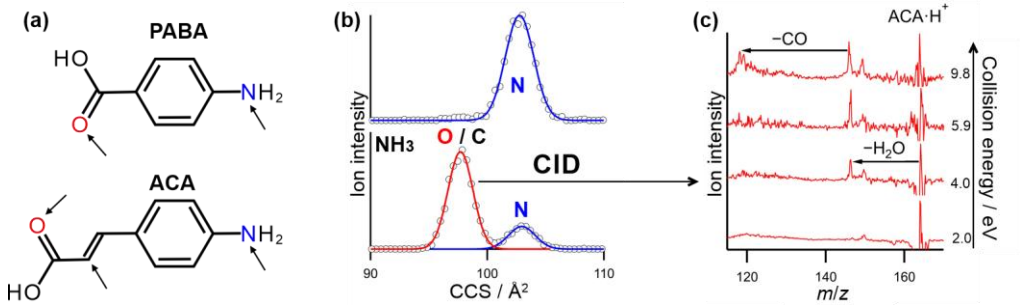

Fig. 1. (a) Structures of PABA and ACA, with arrows indicating the positions where protons are added. (b) Experimental results for ACA·H^+: (top) without reaction gas, (bottom) with NH_3 as the reaction gas. (c) Product ion spectra observed in CID experiments of reaction products of ACA·H^+ + NH_3.

1) K. Ohshimo *et al.*, *J. Phys. Chem. Lett.*, **14**, 8281 (2023).

Structures of Lanthanide Halide Cluster Anions Studied by Ion Mobility Mass Spectrometry: Relationship between Ionic Radius and Geometric Structure due to Lanthanide Contraction

○Yuto Nakajima[1], Patrick Weis[2], Florian Weigend[2], Marcel Lukanowski[2], Fuminori Misaizu[1], Manfred Kappes[2] ([1]Tohoku Univ., [2]Karlsruhe Institute of Technology)

Keywords: *Ion Mobility Spectrometry, Mass Spectrometry, Gas Phase Cluster, Lanthanide Contraction*

Lanthanoid (Ln) complexes are characterized by diverse coordination structures that are influenced by their ionic radii. The ionic radii of lanthanoid(III) ions (Ln^{3+}) gradually decrease from La to Lu, known as the lanthanoid contraction. It is well-established that this systematic reduction in ionic radius leads to diversity in coordination structures, highlighting a relationship between ionic size and coordination chemistry. Rutkowski's previous investigation into the coordination structures of lanthanoid chloride clusters using electrospray ionization (ESI) mass spectrometry and density functional theory (DFT) calculations showed that $La_6Cl_{19}^-$ and $Lu_6Cl_{19}^-$ are classified into different structural classes.[1] This study aims to elucidate the relationship between ionic radii of whole Ln and their cluster structures as coordination models, offering insights into the structural adaptability of lanthanoid systems, which were recently found to play roles in certain bacterial enzymes.[2] Lanthanoid chloride ions were generated by ESI, and their collision cross-sections (CCS) were measured using ion mobility mass spectrometry equipped with cyclic-type ion drift cells.[3] The CCS analysis revealed that $Ln_6Cl_{19}^-$ clusters for Sm–Lu exhibit two distinct components corresponding to different isomers: an octahedral isomer and a prism-like isomer shown in **Fig**. In contrast, smaller clusters such as $Ln_5Cl_{16}^-$ and $Ln_4Cl_{13}^-$ displayed only one component, suggesting a single dominant structural configuration. The relationship between ionic radii and CCS values revealed a turning point in the structural trends of $Ln_5Cl_{16}^-$ and $Ln_4Cl_{13}^-$.

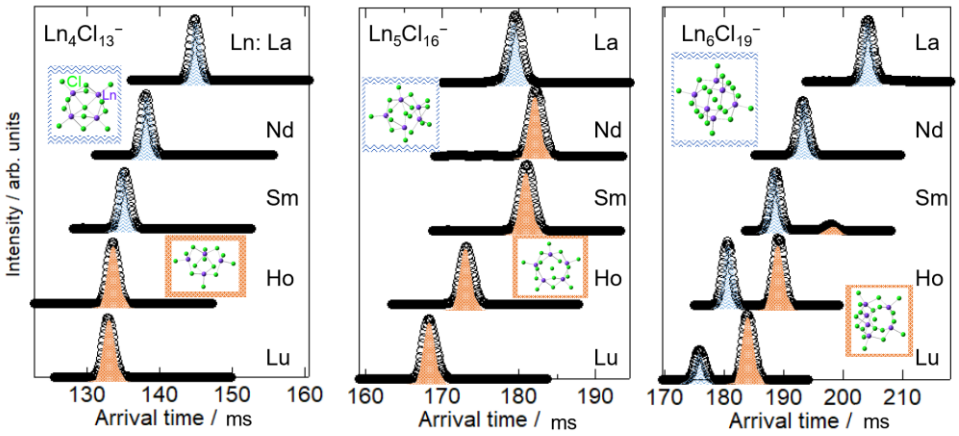

Fig: Arrival time distributions in ion mobility measurements and assigned structures.

1) P. X. Rutkowski et al, *Phys, Chem. Chem. Phys.* **2012**, *14*, 1965. 2) Y. W. Deng et al, *J. Biol. Inorg. Chem.* **2018**, *23*, 1037. 3) Y. Nakajima et al, *Phys. Chem. Chem. Phys.* **2025**, *27*, 1017.

Development of a rapid solution mixing technique using free-impinging liquid-sheet jets

(*Kansai Institute for Photon Science, QST*) ○Tomoyuki Endo, Ryuji Itakura
Keywords: Liquid-sheet jet; Solution mixing; Turbulent flow

Intermediates in chemical reactions driven by solution mixing have been investigated to understand their reaction mechanisms and driving forces. However, the identification of intermediates with lifetimes of a few seconds or less is difficult because of dead time of solution mixing. To achieve rapid solution mixing, a free impinging jet technique has been proposed[1]. In this study[2], we measured mixing time in the free impinging liquid-sheet jets by using a quenching reaction of N-acetyl-L-tryptophan amide (NATA) by N-bromosuccinimide (NBS). Additionally, the theoretical mixing times were calculated by two distinct models assuming laminar and turbulent flows, respectively, to clarify the mixing mechanism in the liquid-sheet jets.

The liquid-sheet jets were formed by impinging two cylindrical jets (φ = 50 μm) of water or ethanol. An ultraviolet pump pulse (λ_{ex} = 266 nm) was irradiated onto the whole area of the liquid-sheet jet to excite NATA. The emission from NATA (λ_{em} = 357 nm) was recorded as a function of the distance from the impinging point with a CMOS camera. NATA was oxidized by NBS to form a non-fluorescent bromohydrin compound.

Emission images of the water/water liquid-sheet jet formed with an NATA aqueous solution (50 μM) and an NBS aqueous solution (8, 16, 32 mM) were normalized by the image taken without NBS to compensate for the non-uniformity due to the spatial distribution of pump pulse intensity. From mono-exponential decay curves of the relative emission intensity as a function of the distance and measured flow speed of the liquid-sheet jet, the mixing time was evaluated to be 36(3) μs. In the case of the water/ethanol liquid-sheet jet, the mixing time was evaluated to be 46(4) μs. Simulations for the laminar flow based on molecular diffusion exhibits a large discrepancy from the experimental results. In contrast, the mixing times in the turbulent flow based on the energy dissipation rate in the impinging area[1,3] were calculated to be 30.3 μs and 51.4 μs for the water/water and water/ethanol jets, respectively, which were in agreement with the experimental results. Thus, the mixing mechanism in the liquid-sheet jet can be explained by turbulent mixing rather than laminar mixing. No clear interface between the water/water and water/ethanol solutions was formed for the present experimental conditions.

The free-impinging liquid-sheet jet technique provides an ultra-thin liquid target, opening a new way for investigating ultrafast electron dynamics using ultrashort laser pulses such as high-order harmonics with attosecond time resolution.

1) R. S. Abiev, and A. A. Sirotkin, *Fluids* ***2020****, 5*, 179. 2) T. Endo, and R. Itakura, *Bull. Chem. Soc. Jap.* **2024***, 97*, uoad021. 3) L. Falk, and J.-M. Commenge, *Chem. Eng. Sci.* ***2010****, 65*, 405.

プラスチック分解物の高選択的かつ高効率な酸化反応を加速させるヘマタイト光電極の設計

（神大院理[1]・神戸大分子フォト[2]）○村尾 智央[1]・隈部 佳孝[2]・立川 貴士[1,2]

Design of hematite photoelectrodes to enhance highly selective and efficient oxidation of plastic degradation products

([1]*Grad. Sch. of Sci., Kobe Univ.*, [2]*Mol. Photosci. Res. Center, Kobe Univ.*)
○Tomochika Murao,[1] Yoshitaka Kumabe,[2] Takashi Tachikawa[1,2]

In recent years, various strategies for utilizing waste plastics have been investigated to address environmental issues. Among them, hydrogen production using photocatalysts and waste plastics has emerged as a promising solution that tackles both environmental and energy problems simultaneously[1)]. In this study, we demonstrated that plastic degradation products can serve as an electron source for photocatalytic hydrogen production. Photoelectrochemical measurements revealed that these degradation products are selectively and efficiently oxidized on a specific co-catalyst supported on hematite photoelectrodes.

Keywords : Photoelectrode; Degradation of plastics; Co-catalysts; Photocatalysts; Hydrogen production

廃プラスチックの利用法は様々に検討されているが、その中でも光触媒と廃プラスチックを用いた水素製造はエネルギー問題をも解決する方法として注目されている[1)]。本研究では、PET 分解反応における生成物のひとつであるエチレングリコール(EG)を水に代わる新たな電子源として利用し、水素製造を行うことを目的とした。Figure 1 に EG 無添加および添加条件で行ったリニアスイープボルタンメトリー測定の結果を示す。Ti ドープされたヘマタイトメソ結晶光電極上に担持された Ni 系助触媒が、EG 酸化反応を選択的に促すことがわかった。また、EG 濃度依存性の実験から、観測された高効率な EG 酸化は触媒表面への吸着力に起因することが示唆された。

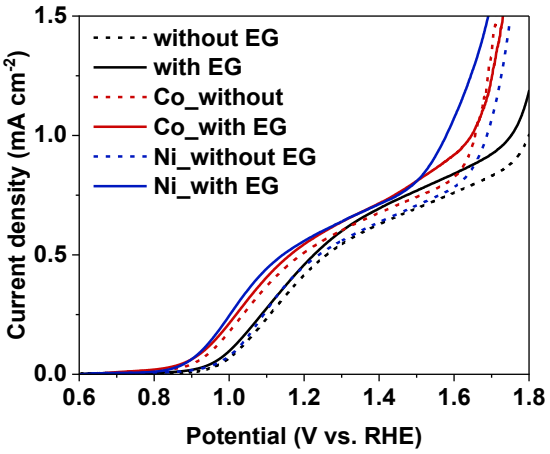

Figure 1. Linear sweep voltammetry (LSV) curves obtained for photoelectrodes with and without co-catalyst in 1 M NaOH in the absence and presence of 100 mM EG.

1) D. Sajwan, A. Sharma, M. Sharma, V. Krishnan, *ACS Catal.* **2024**, *14*, 4865–4926.

ペロブスカイトナノ結晶—シアニン色素間のエネルギー移動における結晶サイズ依存性

(関西学院大生命環境 [1]・関西学院大院理工 [2]) ○山口 哲生 [1]・福増 智也 [2]・久保 直輝 [2]・増尾 貞弘 [1]

Crystal Size Dependence on Energy Transfer from Perovskite Nanocrystals to Cyanine Dyes

([1]*Sch. of Bio. and Environ. Sci.,* [2]*Grad. Sch. of Sci. and Technol., Kwansei Gakuin Univ.*) ○ Tetsuo Yamaguchi,[1] Tomoya Fukumasu,[2] Naoki Kubo,[2] Sadahiro Masuo[1]

Perovskite nanocrystal (PNC) can generate multiple excitons (MX) simultaneously by absorbing multiple photons. The MX annihilated to a single exciton by Auger recombination (AR). In this study, as AR rate is inversely proportional to the PNC size,[1)] we expected that MX can be utilized by deceleration of AR in large sized PNCs. Three types of PNCs with the average edge lengths of 7.9 nm, 12.1 nm and 15.9 nm were synthesized, and multiple energy accepters (Cy3) were adsorbed on the PNCs. Photon correlation functions of the Cy3s were measured with excitation of the PNCs at the single PNC levels. The emitted photon number from the Cy3s on the three sized PNCs increased with increase of the PNC size. It indicates that MX generated in larger sized PNC by a single laser pulse transferred their energy to the multiple Cy3s to emit multiple photons. It suggests the efficient utilization of MX generated in the larger sized PNCs.

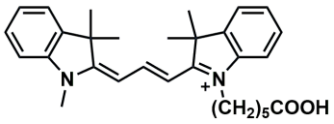

Fig. 1 Molecular structure of Cy3.

Keywords : Energy Transfer, Perovskite Nanocrystal

ペロブスカイトナノ結晶(PNC)は、複数の光子を同時に吸収し、単一 PNC 内に複数の励起子(MX)を生成することができる。しかし、MX は、オージェ再結合(AR)により失活し、単一の励起子になってしまう。本研究では、AR 速度が PNC の体積に反比例することから [1)]、サイズの大きい PNC を活用することで、MX が AR する前にエネルギーを取り出すことができると予想した。そこで、平均粒子径 7.9 nm、12.1 nm、15.9 nm とサイズの異なる 3 種類の PNC を合成し、複数のエネルギーアクセプター(シアニン色素、Cy3)を吸着させることで、MX からのエネルギーの取り出しが可能であるか検討した。

顕微分光法を用いて、単一 PNC レベルで PNC を励起し、Cy3 由来の発光を検出した。光子相関測定により、Cy3 由来の発光光子数を求めたところ、PNC のサイズの増大とともに発光光子数も多くなった。これは、大きい PNC では、単一レーザーパルスにより単一 PNC 内に生成した MX から、表面に吸着した複数の Cy3 にエネルギー移動することで、複数の Cy3 が発光したことを示す。以上のことから、大きいサイズの PNC を用いることで、PNC 内に生成した MX を有効に活用できることを明らかにした。

1) H. Igawashi, M. Yamauchi, S. Masuo, *J. Phys. Chem. Lett.* **2023**, *14*, 2441.

Photophysics of Adenosine Derivatives as Revealed by Liquid Flat Jet Extreme Ultraviolet Time-Resolved Photoelectron Spectroscopy

([1]*Institute of Molecular Science*, [2]*UC Berkeley*) ○Masafumi Koga,[1] Do Hyung Kang,[2] Zachary N. Heim,[2] Daniel M. Neumark[2]

Keywords: *Ultrafast Dynamics*; Photoelectron Spectroscopy; Liquid Flat Jet; DNA Damage

Photophysics and photochemistry of nucleic acid constituents are of fundamental interest in understanding how genetic codes are protected from ultraviolet (UV) light irradiation. The underlying mechanisms of photostability, i.e., the non-destructive dissipation of the excess energy imposed by the UV light absorption, remain elusive even at the single nucleobase level. In this study, femtosecond extreme ultraviolet time-resolved photoelectron spectroscopy (XUV-TRPES) was employed to investigate the relaxation dynamics of adeninosine in aqueous solution. An XUV probe pulse at 21.7 eV can ionize all excited states of a molecule, allowing for full relaxation pathways to be addressed after excitation at 4.66 eV. We also incorporated a gas-dynamic flat liquid jet, which significantly enhanced the pump-probe signal intensity due to the large exposure area (200 μm) of liquid to the incident laser beams compared to a conventionally used cylindrical jet (ca. 30 μm). The obtained TRPE spectra in all systems exhibited signals between 3 and 7 eV electron binding energies. The ultrafast decays within 1 ps were accurately reproduced by the global lifetime analysis under a bi-exponential function with time constants around 100 fs and 500 fs. The decay- associated spectra with a ~500 fs time constant showed distinct peaks 1-eV separated from those at ~100 fs, suggesting that the different electronic state, namely the $n\pi^*$ state, was involved in the relaxation from the initially populated $\pi\pi^*$ state.[1] At the conference site, the ultrafast stepwise relaxation mechanisms depending on the sugar and phosphate groups, and dynamics in adenosine dimer will be discussed.

1) M. Koga, D. H. Kang, Z. N. Heim, P. Meyer, B. A. Erickson, N. Haldar, N. Baradaran, M. Havenith, D. M. Neumark, *Phys. Chem. Chem. Phys.*, **2024**, *26,* 13106.